CHARACTERIZATION OF AN UNINTENTIONAL WI-FI INTERFERENCE DEVICE – THE RESIDENTIAL MICROWAVE OVEN

Tanim M. Taher, Ayham Z. Al-Banna, Donald R. Ucci, Joseph L. LoCicero
Department of Electrical and Computer Engineering
Illinois Institute of Technology
Chicago, IL 60616
Email: tahetan@iit.edu, albaayh@iit.edu

ABSTRACT

Some devices not used for data communications radiate in the 2.4 GHz Wireless-Fidelity (Wi-Fi) band, thus causing unintentional interference that degrades the performance of IEEE 802.11 wireless systems. An analytical model for radio emissions from one of the most common unintentional interferers, the residential microwave oven, is developed from laboratory measurements. Simulation of the analytical model results in a power spectral density and spectrogram that are in good agreement with experimental data. An interference mitigation technique is proposed for the microwave oven emission.

I. INTRODUCTION

The use of the unlicensed Industrial, Scientific, and Medical (ISM) bands [1] has dramatically increased in the last decade. The Federal Communications Commission (FCC) has allocated these bands to permit cost-free wireless communications. The 2.4 GHz band is dominated by high-speed data communications and Wireless Fidelity (Wi-Fi) signals adhering to the IEEE 802.11 standards [2]. Access points, wireless laptops, Personal Digital Assistants (PDAs), Bluetooth devices [3], and cordless phones all intentionally operate in this band for the purpose of communicating. On the other hand, various commercial devices not intended for Wi-Fi communications, like microwave ovens and other residential and industrial products also radiate in the 2.4 GHz band. The emitted electromagnetic Radio Frequency (RF) signals they produce act as interference to Wi-Fi users. The composite interference from intentional Wi-Fi transceivers and unintentional emitters results in reduced network performance, and even connectivity loss.

The appearance of unintentional emitters in the ISM band continues to grow with the advent of high-speed switching electronics. The use of these devices also increases as people continue to purchase a wide variety of home appliances. The interference effect of these devices is detrimental to Wireless Local Area Networks (WLANs) that increasingly permeate our work and living space.

This work was partially supported by the National Science Foundation under contract no. NSF-CNS 0520232.

In this paper, an analytical model is developed for the interference signal from the most common unintentional emitter, i.e., the Micro-Wave Oven (MWO). There are two types of MWOs, residential and commercial. This paper focuses on the residential MWO. An analytical model is valuable when attempting to mitigate the effects of MWO interference on Wi-Fi communications. The model provides information about the spectral signature and the spectrogram of the MWO signal, which are vital for interference mitigation. In general, smart antennas [4] can be used to suppress interference but typically require the spectral signature of the interference signal to effectively mitigate its effect on communication networks. The information available from a spectrogram is useful for mitigation techniques that involve the time-varying characteristics of the MWO signal [5]. Accurately modeling the MWO signal helps develop techniques for WLANs to reliably send data packets even though nearby MWOs are radiating in the ISM band.

This paper is organized as follows. Section II outlines the experimental data and measurements that were used to develop the MWO analytical model presented in Section III. Simulation results that support the analytical model are provided in Section IV. The simulation results are compared with experimental results in Section V. A MWO interference mitigation technique is presented in Section VI followed by conclusions in Section VII.

II. MWO SIGNAL CHARACTERISTICS

In this section, we provide an overview of MWO operation, as well as experimental signal characteristics, that lead to the development of the analytical MWO model. In particular, we explore the frequency-sweeping phenomenon of the MWO signal, the envelope of the MWO signal in the time domain, and the transient signals that exist, but are often overlooked, in the MWO signal.

A. Frequency-Sweeping Phenomenon

The residential MWO contains a single magnetron that periodically turns on and off as the 60 Hz AC line voltage changes from positive to negative [6]. A commercial MWO has two magnetrons that operate 180 degrees out of phase such that energy is always radiated into the MWO

cavity. RF energy leaking from the MWO cavity causes interference in the 2.4 GHz ISM band.

The residential MWO signal, in the ON mode, is similar to a Frequency Modulated (FM) signal [7], with a fixed carrier frequency, and an instantaneous frequency that changes with time. The MWO center frequency varies with the manufacturer and model, but for the models tested, it was in the 2.45 GHz range. The MWO signal is repetitive in nature with a period of 16.67 ms, which is the inverse of the 60 Hz frequency of the AC supply line powering the MWO. However, the frequency-sweep in the MWO signal is less than half of the 60 Hz time period, typically 5-6 ms. This is shown in the spectrogram [8] in Fig. 1, where the sweep of the MWO signal is clearly seen. This figure also shows transients before and after the frequency-sweep. The spectrogram is particularly useful in developing a model for MWO emissions because it experimentally reveals the characteristics of the frequency-sweeping and transient aspects of the MWO signal.

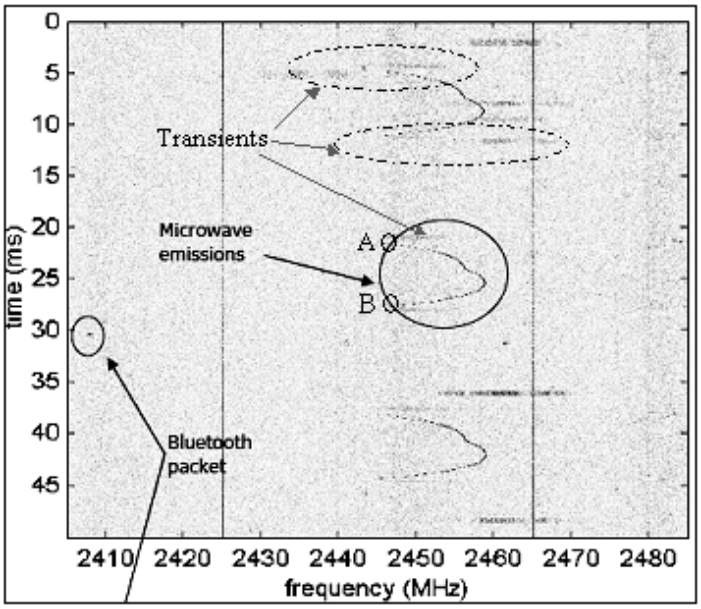

Fig. 1. Spectrogram of the MWO signal
(Courtesy of Stevens Institute of Technology)

During the frequency-sweeping part of the ON cycle, the radiated signal can be characterized as an FM signal with varying power levels. The latter property lends itself to an Amplitude Modulated (AM) mode [7]. Thus, a combined AM-FM waveform will serve as a basis for the frequency-sweeping part of the signal [9]. The approximate sinusoidal shape in Fig. 1 represents the FM signal that sweeps the spectrum over 15 MHz for approximately one half of the 60 Hz AC cycle. A thorough investigation for the amplitude of the MWO signal is detailed in the following subsection.

B. Envelope of the MWO Signal

The envelope of the MWO signal varies significantly during the ON cycle. To study the characteristics of the actual envelope of the MWO signal, measurements were carried out in the Wireless Interference Laboratory (WIL) of Illinois Institute of Technology. The Zero-Span Mode (ZSM) of a Rohde & Schwarz Spectrum Analyzer (model no. FSP 38) was used to capture the envelope of the RF MWO signal. The spectrum analyzer's Resolution Bandwidth (RBW) was set to 10 MHz and the center frequency to 2.455 GHz. The time domain MWO signal captured by the spectrum analyzer is shown in Fig. 2. The amplitude of the MWO signal can be approximated by a sinusoidal waveform when the microwave oven is on. Observe that the oven is on about half of the 60 Hz cycle.

It is important to notice the transient signals at the beginning and end of each ON cycle. These transient signals, together with the frequency-sweeping signal, comprise the radiated MWO signal. The transient signals are studied in detail in the following subsection.

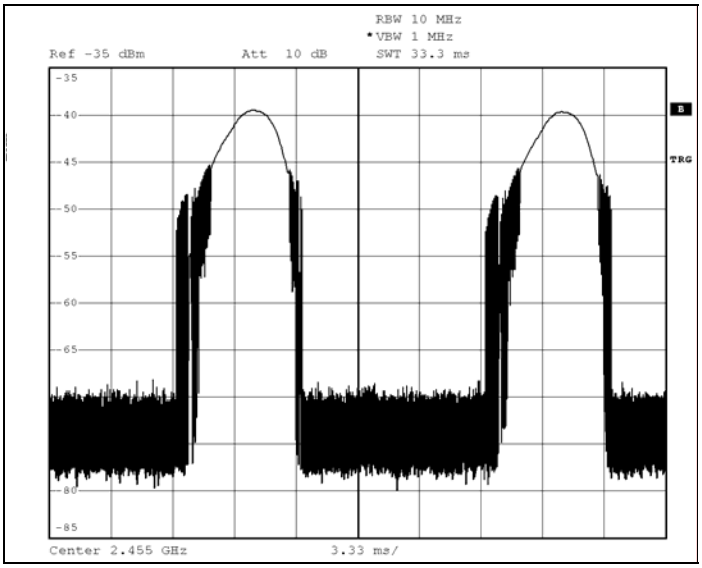

Fig. 2. The envelope of the MWO signal over two 60 Hz cycles (3.33 ms/div)

C. Transient Part of the MWO Signal

The transient part of the MWO was observed in Fig. 2. Figure 1 also shows these transient signals, one occurring at the beginning and another occurring at the end of the ON cycle of the MWO. The characteristics of the transient signals in the time and frequency domains are further investigated here. Numerous ZSM measurements were taken to estimate the bandwidth of the transient signal as well as its duty cycle. The ZSM captures were obtained at different frequencies across the ISM band, using a narrow resolution bandwidth of 10 kHz. If a periodic transient

signal was detected at that ZSM center frequency, then its power and duty cycle were measured.

To synchronize all the ZSM captures of the transient signal at different frequencies, a 60 Hz line trigger was used. With this experimental setup, the zero-span captures of the transient signals at different frequencies are aligned. This is illustrated in Fig. 3 where the periodic transient signals are at the same time locations, even though the capturing frequencies are different (2.46 GHz and 2.44 GHz). Observe that the width of these transient signals is approximately 1 ms at both the frequencies in Fig. 3, with the turn-on transient slightly longer than the turn-off transient.

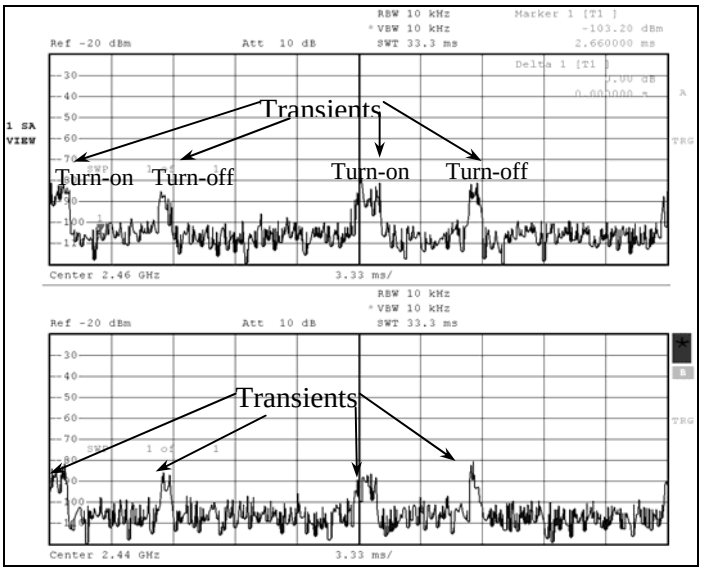

Fig. 3. Zero-span measurements at 2.46 GHz and 2.44 GHz over two 60 Hz cycles (3.33 ms/div)

A programmed spectrum analyzer captured a series of ZSM measurements at uniformly spaced frequencies over the 85 MHz ISM band to estimate the bandwidth of the turn-on and turn-off transients. Measuring the periodic time-varying power signatures of the transient signal over the 2.4 GHz ISM band and combining all the zero-span captures, an experimental spectrogram was generated showing the transient signals. The contour plot of the spectrogram is shown in Fig. 4 over one power cycle with the low-level noise suppressed. The transient signals are broadband, extending over 60 MHz in bandwidth. Also, the power of the transient signals is concentrated at frequencies where the sweeping part of the MWO signal meets the transient part in the spectrogram plot (see points A and B in Fig. 1).

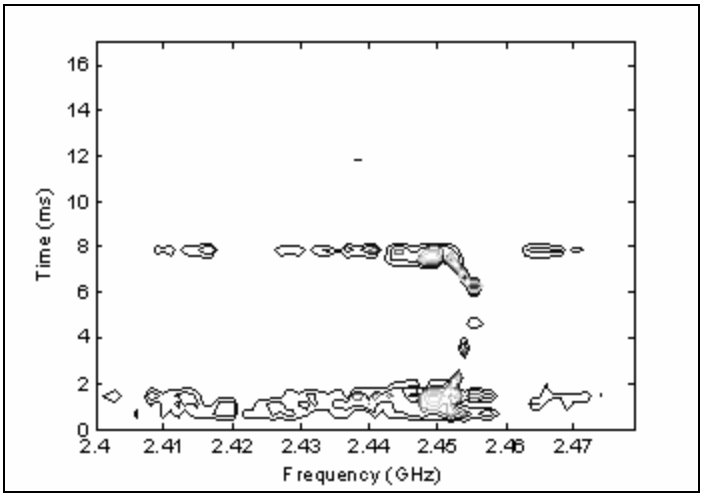

Fig. 4. An experimental spectrogram for transient signals over one 60 Hz cycle (2 transient signals)

It is useful to understand why the transients occur in the MWO. The MWO magnetron needs a minimum threshold voltage (Volt A, Fig. 5) to operate, i.e., to emit microwave energy. Since Volt A is positive, the time duration for the ON cycle is less than that of the OFF cycle. This is observable in Figs. 1-4.

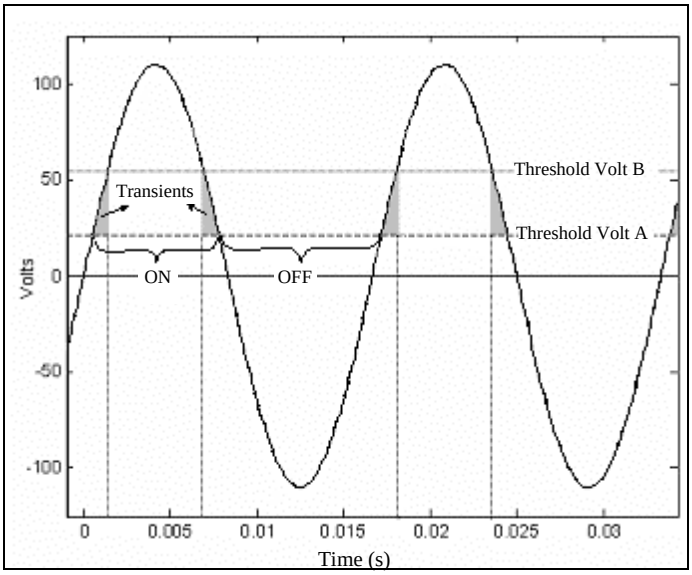

Fig. 5. MWO signal generation process

The minimum threshold voltage (Volt A) is inadequate for sustained operation of the magnetron. A second threshold (Volt B > Volt A) is required for the MWO to generate a frequency-sweeping signal. Between the two thresholds, the MWO emits wideband transient pulses. The transient areas are shown in Fig. 5. The threshold values and the transient times are manufacturer dependant, with a nominal transient duration of 1 ms. Obviously, transients are periodic and synchronized to the AC line signal.

III. ANALYTICAL MODEL OF MWO SIGNAL

From the experimental data and analysis in the previous section, an analytical model can be developed. The MWO signal can be expressed as the sum of two wideband transient signals and a frequency-swept signal during ON cycle, and zero during the OFF cycle. The frequency-swept signal is modeled as an AM-FM signal. Based on the shapes of the MWO signals in Figs. 1 and 2, the frequency-swept signal, $s(t)$, is modeled as a sinusoidally modulated FM signal with a sinusoidally shaped amplitude, $x(t)$. Here, both the modulations are at the 60 Hz line frequency.

The 1 ms (approximate) transient signal pulse was modeled as the sum of two sinc waveforms modulated at different carrier frequencies. The two sinc pulses also have different main lobe widths in the time domain, and thus different bandwidths in the frequency domain. One sinc waveform has a wide spectral bandwidth to provide power across the entire ISM band, while the other sinc waveform has a narrower bandwidth with power concentrated in the frequency-swept band. The transient bandwidths are 40-80 MHz and the main lobe of each sinc waveform is in the order of nano-seconds. Figure 6 shows a qualitative plot of the time domain locations of these signals for each ON cycle.

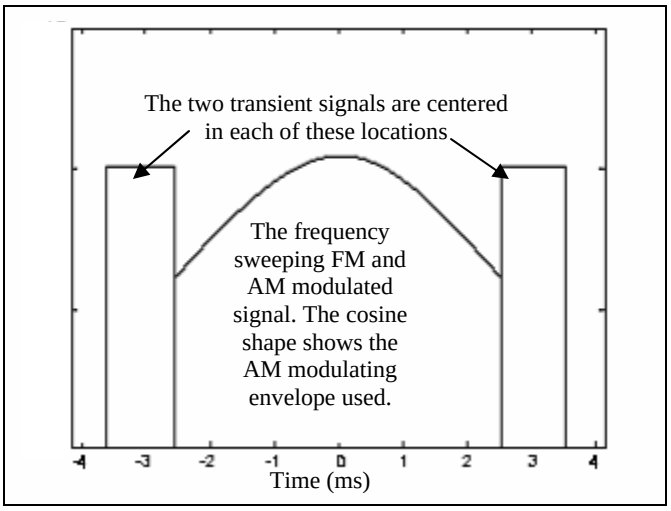

Fig. 6. Qualitative representation of MWO signal model

The complete MWO signal, $v(t)$, can be expressed as the sum of ON cycle wave-shapes, $c(t)$, that is,

$$v(t) = \sum_{n=-\infty}^{\infty} c(t - nT) \ , \tag{1}$$

where $T = 1/f_{ac}$ and $f_{ac} = 60$ Hz.

Using the structure shown in Fig. 6 and the signal description above, the ON cycle wave-shape can be written as,

$$\begin{aligned} c(t) = {} & A_1 p(t + t_a; b_1) \cos(2\pi f_1 t) \\ & + A_2 p(t + t_a; b_2) \cos(2\pi f_2 t) \\ & + s(t) \\ & + A_1 p(t - t_a; b_1) \cos(2\pi f_1 t) \\ & + A_2 p(t - t_a; b_1) \cos(2\pi f_2 t), \end{aligned} \tag{2}$$

where the pulse waveform, $p(t)$, is,

$$p(t; b) = \mathrm{sinc}(bt), \ \ |t| < 0.5T_p, \tag{3}$$

The power in the transient pulses is dictated by the amplitudes, A_1 and A_2, and the center of their spectra is determined by the carrier frequencies, f_1 and f_2. The time locations of the transient pulses are at $\pm t_a$ and their duration is T_p. The bandwidths of the two transients are determined by b_1 and b_2.

The AM-FM signal, with sinusoidal modulation, can be written as,

$$s(t) = A\, x(t) \cos\left(2\pi f_c t + \beta \sin(2\pi f_{ac} t)\right), \ |t| < 0.5T_s, \tag{4}$$

where the amplitude variation is given by,

$$x(t) = \cos(2\pi f_{ac} t). \tag{5}$$

The power in $s(t)$ is dictated by the amplitude A and the sweep time, T_s. The peak frequency deviation is determined by the modulation index, β, while T_s and β together determine the frequency-swept band. The center frequency of the magnetron is given by f_c.

Using the model, any MWO signal can be represented by a total of 12 parameters. It is, of course, possible to refine the model with different pulse widths for the turn-on and turn-off transients, non-symmetric pulse locations, and other pulse shapes. However, the 12 parameter model, when simulated, provides very good agreement to experimental measurements as detailed in the next section.

IV. SIMULATION RESULTS

The analytical model presented in the previous section was simulated using MATLAB®. The simulations were carried out in the MHz and kHz ranges for computational convenience. Our simulations have shown that this analytical model is scalable to all frequencies and bandwidths as the general characteristics of the Power Spectral Density (PSD) and the spectrogram are preserved. Figure 7 shows the PWelch [10] PSD estimate for one simulation run, and Fig. 8 shows its spectrogram. Here, the FM carrier frequency was set to 1 MHz and the FM sweep bandwidth was set to 0.05 MHz. In this simulation, the transient bandwidths are each 0.05 MHz, and the

transient carrier frequencies, f_1 and f_2, are chosen so that both spectra span a 0.1 MHz range.

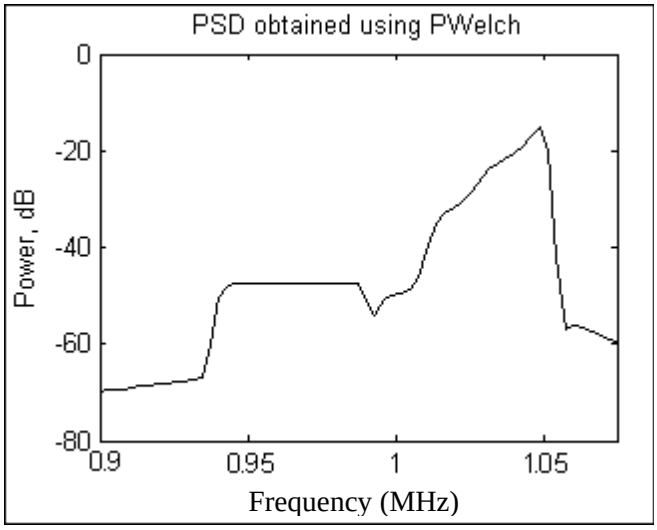

Fig. 7. Simulated PSD of the MWO signal (carrier frequency in 1 MHz range)

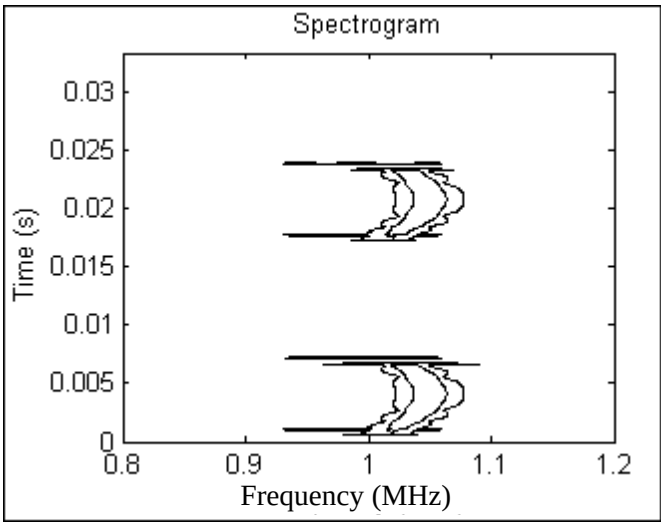

Fig. 8. Simulated spectrogram of the corresponding MWO signal (carrier frequency in 1 MHz range)

In a second simulation, the FM carrier frequency was set to 100 kHz, the sweep bandwidth was fixed at 10 kHz and the total transient bandwidth was set at 20 kHz. The PSD and the spectrogram are displayed in Figs. 9 and 10, respectively. In this case, the wide transient bandwidth was 20 kHz and the narrow transient was 10 kHz. Here f_2 was set so that the narrow transient signal's spectrum overlapped with frequency-swept band.

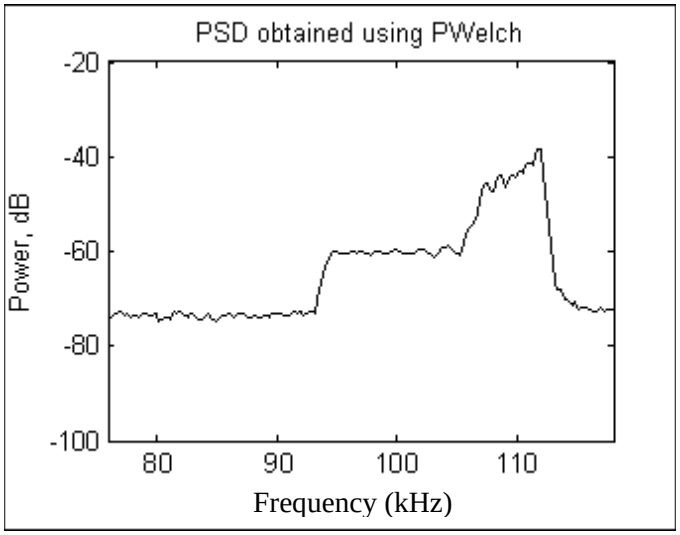

Fig. 9. Simulated PSD of the MWO signal (carrier frequency in 100 kHz range)

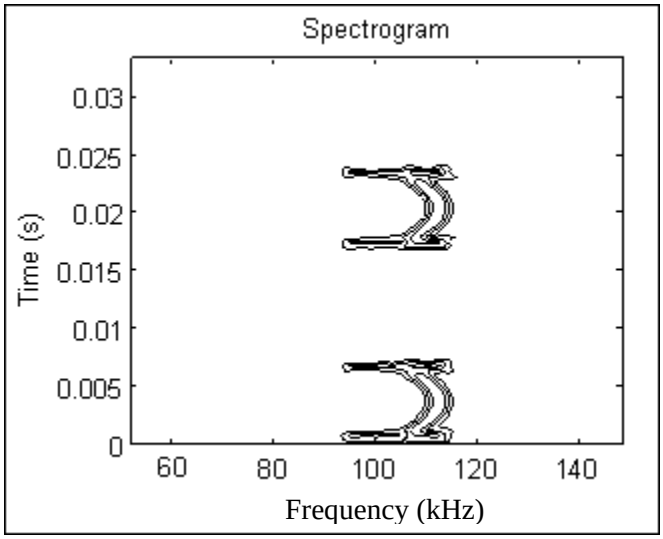

Fig. 10. Simulated spectrogram of the corresponding MWO signal (carrier frequency in 100 kHz range)

V. COMPARISON OF ANALYTICAL AND EXPERIMENTAL SPECTRAL SIGNATURES

Figure 11 shows the PSD of an actual MWO, experimentally measured in the WIL. Similar characteristics were observed for other MWOs whose spectra were measured. Comparing Fig. 11 with Figs. 7 and 9, we see that the simulation results, for the analytical model introduced in section III, capture the main features of the actual MWO PSD. The maximum power is concentrated at the higher frequencies in the frequency-swept region. The power in the lower frequencies comes from the transients and is 25 dB weaker in strength. This reduced PSD level is seen both in experimental and simulated results. The simulated spectrograms in Figs. 8 and 10 compare quite well with the experimental spectrogram shown in Fig. 4. In particular, the transient

signatures of the experimental and simulated MWO signals are very similar.

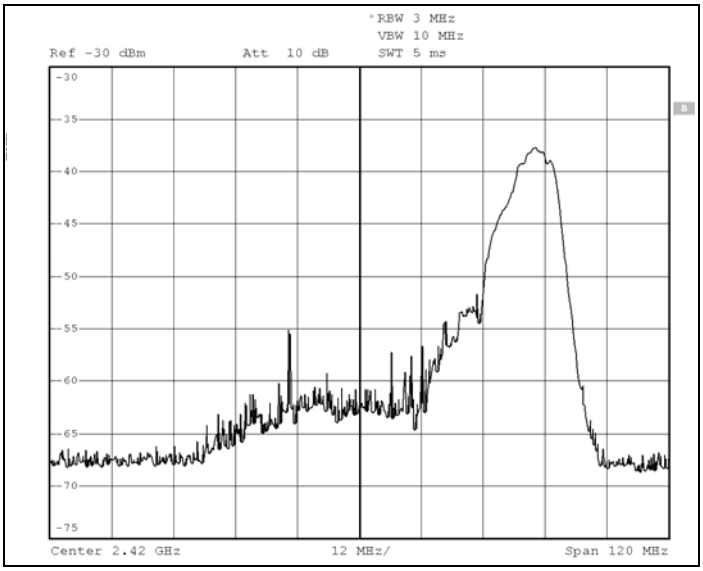

Fig. 11. Experimental PSD for a MWO (center 2.42 GHz, 12 MHz / division)

VI. INTERFERENCE MITIGATION

In this section, a technique that allows Wi-Fi devices to avoid interference caused by MWO signals is outlined. From above, it was seen that the frequency-swept part of the MWO signal spans a relatively narrow bandwidth (approximately 15 MHz). The transient signal bandwidths are much larger (60 MHz or more) and they occupy the entire ISM band. Due to this relatively large bandwidth, the MWO affects data communications in all 802.11 channels [11]. However, the transient bursts are periodic. Thus, if the transient time locations are known, then MWO interference can be avoided by simply stopping data transmission during those time intervals.

Consider the case in which an 802.11 signal is being transmitted at channel 1, centered at 2.412 GHz, with a main-lobe bandwidth of 22 MHz [2]. The MWO frequency-swept spectrum does not impinge on channel 1, so we can freely operate in this channel during the OFF cycle, and during the time interval when the MWO emits the AM-FM signal. Since the transient signals exist for only 2 ms out of the 16.67 ms period, then in theory, 88% of the time, MWO interference can be avoided in channel 1.

Now, consider the case when another common 802.11 channel is being used, that is, channel 11, which is centered at 2.462 GHz. The MWO frequency-swept signal and the transient pulses both interfere with this channel. However, during the OFF cycle, that is 50-60% of the time, the MWO signal interference can be avoided while transmitting in channel 11. For each 802.211 channel and MWO spectral signature, an effective interference mitigation paradigm can be formulated.

For MWO interference mitigation, the Wi-Fi transmission device must be synchronized with the AC line signal. For Wi-Fi devices with AC power, the synchronization is relatively easy to achieve. Once synchronized, the position of the transient pulses can be estimated from the zero crossings of the AC voltage, the average duration of the transient pulses, and the average frequency-sweep time. For the Wi-Fi devices that are battery-powered, synchronization can be done by using the 60 Hz periodic transient bursts of the MWO signal that are detectable throughout the ISM band.

To implement MWO emission mitigation, the Wi-Fi device simply requires a detector that uses the signature of the MWO interference signal to identify when a MWO is operating. The MWO interferer is present when there is a 60 Hz periodic signal in the ISM band, synchronized with the AC line voltage. If the Wi-Fi device is using channel 11, it can switch to a channel outside the frequency-swept band, like channel 1, or employ a mitigation mode where it only transmits during the OFF cycle duration. Any Wi-Fi device operating on channel 1 (or on other channels outside the frequency-swept region) can transmit data in the manner shown in Fig. 12. That is, it transmits at all times other than when the transients are present.

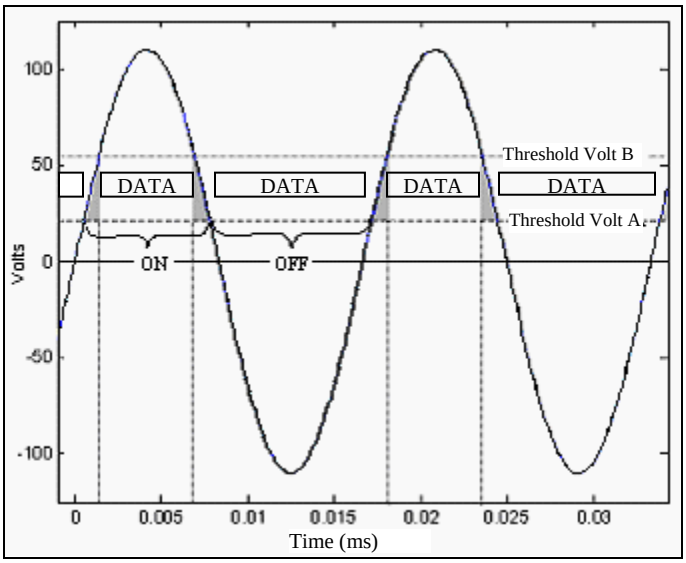

Fig. 12. Data transmission using 802.11 channel 1 (shaded areas are transient locations)

VII. CONCLUSION

The microwave oven signal as an unintentional emitter in the 2.4 GHz ISM band was investigated in this paper. An analytical model was developed and supported by simulation results and experimental data, specifically the PSD signature and the spectrogram. The model introduced here is useful in developing interference mitigation techniques. An interference mitigation technique has been proposed to enable Wi-Fi devices to reliably transmit data during the presence of MWO interference.

ACKNOWLEDGEMENTS

We would like to thank Mr. Theodoris Kamakaris, Dr. Uf Tureli and Dr. Patrick White from the Wireless Network Security Center at Stevens Institute of Technology for providing the spectrogram plot in Fig. 1. We also would like to thank Mr. John MacDonald at Illinois Institute of Technology for his assistance with the ZSM measurements.

REFERENCES

[1] R.J. Bates, D.W. Gregory, *Voice & Data Communications Handbook (Standards & Protocols)*, 4th ed. New York, NY: McGraw Hill, 2001.

[2] IEEE standard 802.11: "Wireless LAN Medium Access Control (MAC) and Physical Layer Specifications," IEEE standard for Information Technology (June 1997).

[3] M. Guizani, "Bluetooth: A Survey on the Technology and Security," *China Communications*, vol. 1, no. 1, pp. 75-80, Dec. 2004.

[4] R.T. Compton, Jr., *Adaptive Antennas: Concepts and Performance*. Upper Saddle River, NJ: Prentice Hall, 1988.

[5] Avaya Wireless Based LANs Course, URL: http://wireless.ictp.trieste.it/school_2002/lectures/ermanno/interference.ppt

[6] A. Kamerman, N. Erkocevic; "Microwave Interference on Wireless LAN's Operating in the 2.4 GHz ISM Band", in *Proceedings of IEEE PIMRC Conference*, 1997, vol. 3, pp. 1221-1227.

[7] J. Proakis, M. Salehi, *Communications Systems Engineering*, 2nd ed. Upper Saddle River, NJ: Prentice Hall, 1994.

[8] Wireless Network Security Center, Stevens Institute of Technology, web-site URL: http://www.winsec.us/new/docs/NSF-nfocom05.pdf

[9] Y. Zhao, B.G Agee, J.H. Reed; "Simulation and Measurement of Microwave Oven Leakage for 802.11 WLAN Interference Management", in *Proceedings IEEE International Symposium on Microwave, Antenna, Propagation and EMC Technologies for Wireless Communications,* Beijing, China, 2005.

[10] J. Proakis and D. Manolakis, *Digital Signal Processing: Principles, Algorithms and Applications*, 3rd ed. Upper Saddle River, NJ: Prentice Hall, 1996.

[11] P.E. Gawthorp, F.H. Sanders, K.B. Nebbia and J.J. Sell, NTIA Report 94-303-1; "Radio Spectrum Measurements of Individual Microwave Ovens" – Volume 1, 1994.